Asian Journal of Water, Environment and Pollution, Vol. 19, No. 1 (2022), pp. 73-79.
DOI 10.3233/AJW220011

Modeling the Effect of Magnesia Nanoparticles on CO Hydrogenation to Light Olefins in a Continuous Flow Reactor Using Fine Gaussian Support Vector Machine

Alyaa K. Mageed, Mohamed A. Abdel Ghany, May Ali Alsaffar* and Jamal M. Ali
Department of Chemical Engineering, University of Technology, Iraq
✉ mayrashid1973@gmail.com

Received June 27, 2021; revised and accepted July 19, 2021

Abstract: The effect of utilising energy derived from fossil sources on the environment has aroused research interest in alternative and sustainable energy sources. Synthesis gas, a mixture of carbon monoxide (CO) and hydrogen can be used as starting materials in hydrogenation reactions to produce chemical intermediates that can be used in various processes. This study investigates the robustness of applying a fine Gaussian support vector machine algorithm for predicting light olefins from catalytic CO hydrogenation using magnesia nanoparticles-based catalysts. The datasets obtained from the CO hydrogenation reaction consist of input parameters such as magnesia nanoparticles contents, reaction temperature, and reactor pressure, and the output parameters which include CO conversions and the selectivity of light olefins (CH_4, C_2H_6, C_2H_4 C_3H_8, C_4H_8, and C_3H_6). The dataset was trained and employed for the prediction of the light olefins using a support vector machine with an inbuilt Fine Gaussian Kernel function. The performance of the support vector machine was evaluated using the coefficient of determination (R^2), root mean squared error (RMSE), mean square error (MSE), and the mean absolute error (MAE). The support vector machine showed significant potential in the prediction of CO conversion, CH_4 selectivity, C_2H_6 selectivity, and C_2H_4 selectivity as indicated by R^2 of 0.770, 0.800, 0.730, and 0.930, respectively. While less predictive performance was obtained for the prediction of C_3H_8 selectivity, C_4H_8 selectivity and C_3H_6 selectivity as indicated by R^2 of 0.630, 0.610, and 0.320, respectively.

Key words: Support vector machine, CO hydrogenation, syngas, magnesia nanoparticles, light olefins.

Introduction

The increasing concern in environmental pollution and the need for sustainable production has propelled research efforts in the direction of finding viable solutions to alternative means of production with less impact on the environment (Azapagic et al., 2016). In view of this, several technological pathways have been investigated as robust alternatives for the production of sustainable and environmentally friendly products (Rădulescu et al., 2009). One of such technological processes is carbon monoxide (CO) hydrogenation which entails the catalytic conversion of synthetic gas, a mixture of CO and hydrogen to light olefins (Mohammadi et al., 2021; Zhu et al., 2017). Light olefins consist of short-chain hydrocarbons (C_nH_{2n}) such as ethylene, propylene, butenes, and butadiene that can be employed as building blocks in the petrochemical industries to manufacture a wide range of products (Corma et al., 2017). The conventional means of producing olefin in a large-scale process entail the utilisation of crude oil in the catalytic cracking reaction.

*Corresponding Author

However, this process faces several challenges such as coils coking, and limited product flexibility as reported by Corma et al. (2017). CO hydrogenation is an emerging process for light olefin production and offers the advantage of utilising a more environmental feedstock as well as wide product flexibility (Pedersen et al., 2018).

The production of light olefin by catalytic CO hydrogenation has been widely reported in the literature. The performance of photothermal CO hydrogenation to olefins using MnO modified Ni catalysts has been reported by Wang et al. (2020). The study revealed that the MnO modified Ni catalysts were very effective in the CO hydrogenation reaction and displayed a high selectivity towards light olefins with negligible CO_2. In a similar study, Shi et al. (2020) employed Mn-doped ferrites for CO hydrogenation to light olefins. The performance of the Mn-doped ferrites in the CO hydrogenation resulted in high selectivity (54.4%) of light olefin compared to 33% reported by Wang et al. (2020). It can be inferred that the Mn-doped ferrites catalyst has a higher selectivity towards light olefin in CO hydrogenation compared to the MnO modified Ni catalysts. The promotional effect of Mn on Fe-Mn bimetallic catalysts in CO hydrogenation to light olefin has been reported by Yang et al. (2021). Unlike the MnO modified Ni catalyst and Mn-doped ferrites catalysts, the Mn-doped Fe-Mn bimetallic catalysts display a high selectivity of 60.6%, which can be attributed to the synergistic effect of the Fe and Mn catalysts. Besides investigating the performance of various catalysts in CO hydrogenation reaction, the effect of various parameters on the reaction has been reported. Mohammadi et al. (2021) employed response surface methodology for the optimisation of various operating parameters in CO hydrogenation to light olefins. The CO hydrogenation reaction resulted in maximum CO conversion and light olefin under optimum conditions of 3.21 bar, 290^{o}C and 1.85 for pressure, temperature, and H_2/CO ratio, respectively. In a similar study, Atashi et al. (2013) employed the response surface methodology to optimise CO hydrogenation to light olefin. The study revealed that the catalyst substantially affects the CO hydrogenation. Under optimised conditions, high selectivity towards light olefins such as ethane, propane, propylene, butylene was obtained.

Experimental studies often resulted in the generation of a huge amount of data which can be utilised for modeling the non-linear relationship between the process parameters and the outputs. To achieve this, supervised machine learning algorithms such as support vector machines can be employed. Support vector machine possesses in-built algorithms that can be employed for classification and regression learning (Bai et al., 2019). Support vector machine has been utilised for modeling various processes (Fan et al., 2018; Zendehboudi et al., 2018). Leong et al. (2021) employed a support vector machine for the prediction of the water quality index. A robust prediction of the water quality index was achieved with a high coefficient of determination (R^2) of 0.9184. Also, the application of a support vector machine for modeling the prediction of dissolved oxygen concentration in a hypoxic river system has been reported by Ji et al. (2017). With an R^2 of 0.8646, the support vector machine displayed a high tendency in learning the relationship between the input variables and the model output. Yuan et al. (2017) reported a robust prediction of wind power using a support vector machine. The modeling of the prediction of CO conversion and selectivity during CO hydrogenation reaction by support vector machine has not been reported in the literature. This study, therefore, aimed to employ a support vector machine for modeling the prediction of the effect of magnesia nanoparticles on the catalytic hydrogenation to light olefins.

Experimentation and Modeling Strategy Using Support Vector Machine

The data employed for the modeling consist of input parameters such as the pressure of the reactor, the reaction temperature, and the magnesia contents in the catalyst. While the output consists of CO conversion, CH_4 selectivity, C_2H_6 selectivity, C_2H_4 selectivity, C_3H_8 selectivity, C_4H_8 selectivity, and C_3H_6 selectivity. The detailed experimental design using the Box-Behnken method and the CO hydrogenation reaction have been reported by Atashi et al. (2013). The catalytic CO hydrogenation was performed in a continuous flow tubular reactor that consists of the catalysts supported with quartz wool. The temperature of the reactor was regulated using a temperature controller. In order to improve the catalytic activity, the catalyst was reduced in situ in a flow of 60 mL/min of H_2/N_2 (1:1) for 2 h at 400^{o}C. Subsequently, the reacting and the carrier gases, which consist of CO, H_2, and N_2, were allowed to flow into the reactor with their flow rate being regulated using a mass flow meter. The product compositions were analysed using an online gas chromatography.

The detailed steps involved in the application of the support vector machine are depicted in Figure 1. The

support vector machine is incorporated with a function approximation ability that enables it to handle a non-linear process. The inbuilt kernel functions such as the polynomial, exponential radial basis function, radial basis function, sigmoid and linear can be employed to improve the performance of the support vector machine regression model that provides a better generalisation. The dataset which consists of the input parameters (reactor pressure, reaction temperature, magnesia content) and the output parameters (CO conversion and the light olefins selectivity) was divided into three portions for training, testing, and validation in the proportion of 0.7, 0.15, and 0.15, respectively to prevent overfitting. The dataset was pre-processed in an excel sheet and subsequently uploaded into a regression learning environment in MATLAB 2020b (MathWorks Inc.). The Fine Gaussian was selected as a kernel for the support vector machine used in the modeling process. The dataset was strained and the performance of the support vector machine model in predicting the CO conversion and the light olefins was evaluated using R^2, root mean squared error (RMSE), mean squared error (MSE) and mean absolute error (MAE).

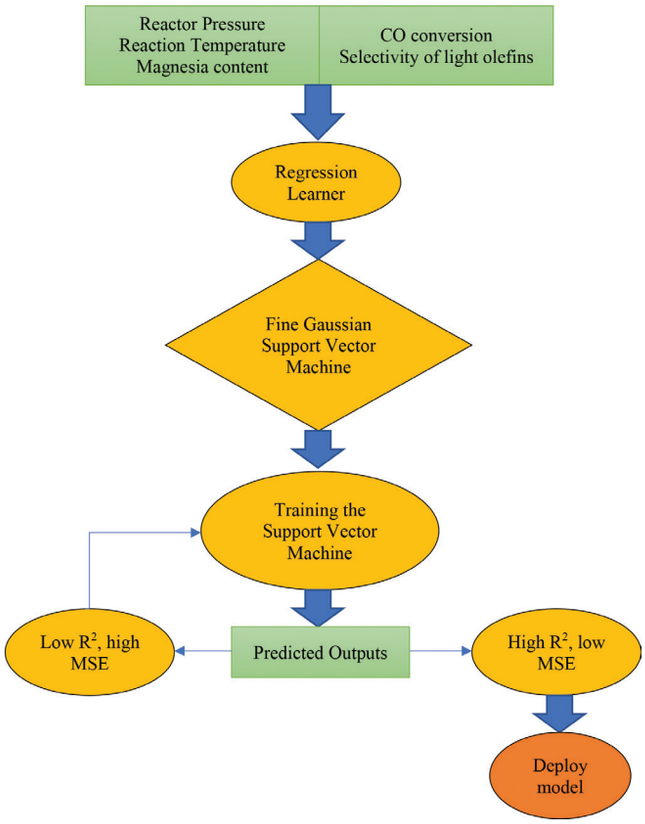

Figure 1: Process flow for the support vector modeling the CO hydrogenation.

Results and Discussion

The interaction analysis as a function of the effects of the various parameters on the olefin with the highest selectivity is represented in Figure 2. As revealed by Figure 2 (a), the relationship between the reaction temperature, magnesia contents, and CH_4 selectivity is non-linear. An increase in the reaction temperature resulted in a corresponding increase in the CH_4 selectivity until it attained a maximum value of 57%. On the contrary, the increase in the magnesia contents led to an increase in the CH_4 selectivity which attained its peak at a magnesia content of 15%. This could be attributed to the fact that magnesia contents > 15% resulted in the deactivation of the catalyst. As shown in Figure 2 (b), an increase in both reactor pressure and magnesia content resulted in a decrease in the CH_4 selectivity. It can be seen that high selectivity is favoured at reactor pressure < 4 bar and magnesia content < 15%. A similar trend is observed in Figure 2 (c) for the effect of the reactor pressure and temperature on the CH_4 selectivity.

The comparison between the actual and predicted CO conversion in the hydrogenation reaction is depicted in Figure 3. The combination of the three parameters in the experimental design produces variation in the CO conversion during the hydrogenation reaction. The lowest CO conversion of 7.84% is observed using 25wt% magnesia nanoparticles, at 280°C and reactor pressure of 4 bar. While the highest CO conversion of 53.03% is obtained at 15wt% magnesia nanoparticles, at 380°C and 7 bar. This implies that a high CO conversion is favoured using mild magnesia nanoparticles, a temperature of 380°C and high pressure. The predicted CO conversion is consistent with actual values at each datapoint. However, the R^2 of 0.770 obtained from the prediction indicates that only 77% of the dataset can be learnt using the Fine Gaussian Support Vector Machine algorithms. The predicted error of 15.018% measured by the MSE indicates that algorithms can further be improved to obtain more accurate predictions.

Figure 4 shows the dispersion plots of the actual and predicted CH_4 selectivity, C_2H_6 selectivity, and C_2H_4 selectivity. Also, it can be seen that the combination of the three parameters has varying effects on the light olefin selectivity. As shown in Figure 4 (a), the magnesia nanoparticles had significant effects on the selectivity for each data point. The least CH_4 selectivity of 44.5% was obtained using 1wt% magnesia nanoparticles, reaction temperature of 330°C, and reactor pressure of 1 bar. While the highest CH_4 selectivity of 60.2% was obtained using 15wt% magnesia nanoparticles, reaction

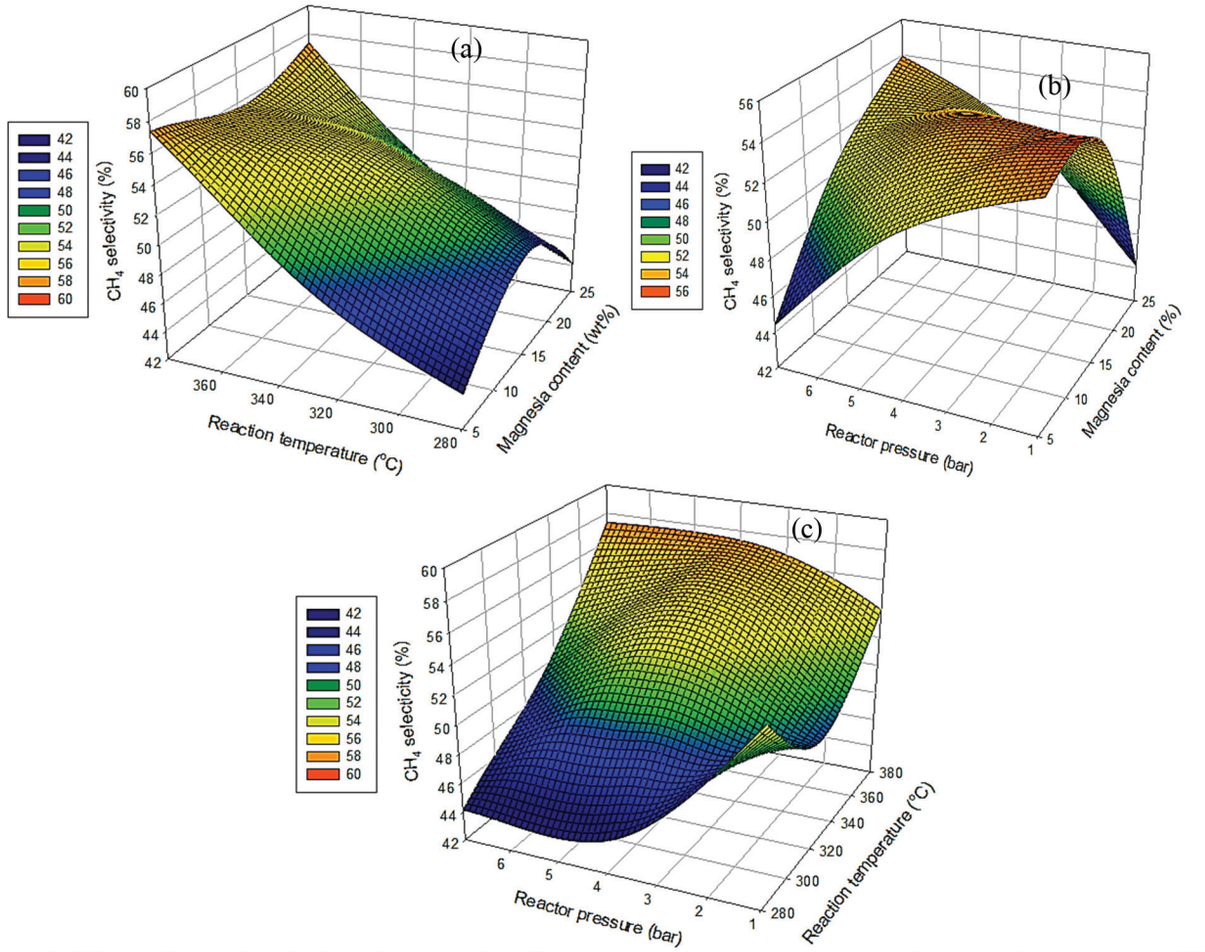

Figure 2: Three-dimensional plots showing the effect (a) reaction temperature and magnesia content on CH_4, (b) Reactor pressure and magnesia content and (c) Reactor pressure and Reactor temperature on CH_4 selectivity.

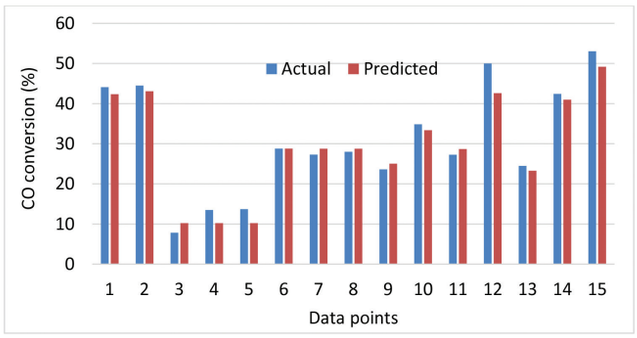

Figure 3: Dispersion plots showing the comparison between the actual and predicted CO conversion.

temperature of 380°C, and the reactor pressure of 7 bar. For most of the data points, the predicted CH_4 selectivity is consistent with the actual values. The R^2 of 0.800 obtained from the model prediction indicated that the support vector machine using a fine Gaussian kernel can only learn 80% of the dataset with a prediction error of 10.830% as calculated using the MSE. Although, the support vector machine algorithm shows great potential in predicting the CH_4 selectivity, however, the algorithm can further be optimised for better predictability. Unlike the CH_4 selectivity that was highly favoured at all the data points, the selectivity of the C_2H_6 significantly varies with the combined parameters at each data point. The lowest C_2H_6 selectivity of 1.7% was obtained at 15wt% magnesia nanoparticles, reaction temperature of 280°C, and reactor pressure of 1 bar. While the highest C_2H_6 selectivity of 13.4% was obtained using 5wt% magnesia nanoparticle, reaction temperature of 330°C, and reactor pressure of 7 bar. The prediction of the C_2H_6 selectivity resulted in R^2 of 0.730 indicating that 73% of the dataset can be learned by the support vector machine algorithm with a prediction of 3.266% obtained from the MSE. Also, Figure 3 (c) shows the dispersion plots for the comparison between the actual and the predicted C_2H_4 selectivity obtained from the

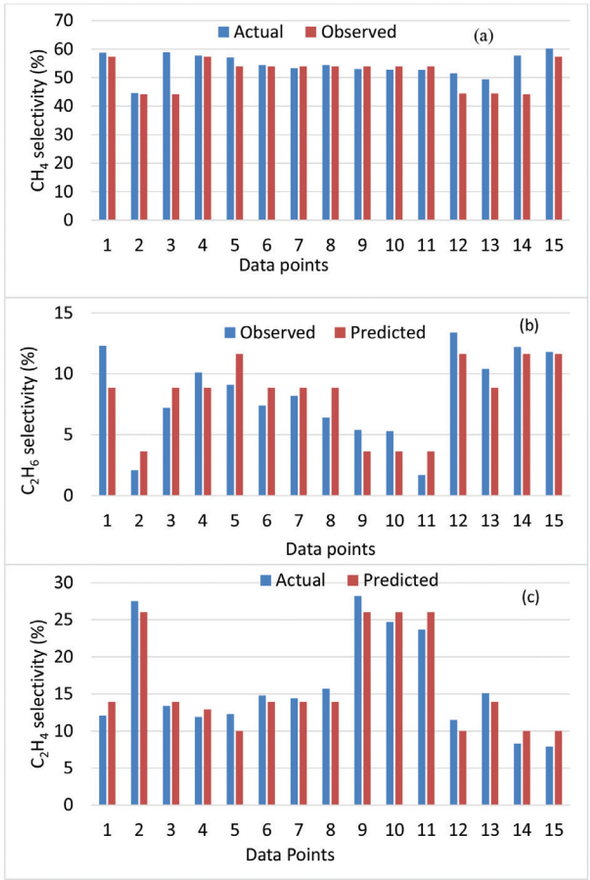

Figure 4: (a) The actual and predicted CH_4 selectivity, (b) the actual and predicted C_2H_6 selectivity and (c) the actual and predicted C_2H_4 selectivity.

CO hydrogenation. Like the C_2H_6 selectivity, the C_2H_4 selectivity is unevenly distributed along with the data points due to the differences in the combined parameters. The highest C_2H_4 selectivity of 28.2% was obtained using 5wt% magnesia nanoparticles, reaction temperature of 330 ^oC, and reactor pressure of 1 bar. The predicted C_2H_4 selectivity is consistent with the actual values as indicated by the highest R^2 of 0.930. This implies that the support vector machine can learn over 93% of the dataset with a prediction error of 2.809%.

Figure 5 shows the dispersion plots of the actual and predicted C_3H_8 selectivity, C_3H_6 selectivity and C_4H_8 selectivity. It can be seen that there are variations in the C_3H_8 selectivity, C_3H_6 selectivity, and C_4H_8 selectivity along with the data points. As shown in Figure 5 (a), the C_3H_8 selectivity is unevenly distributed along with the data points due to the variation in the combined parameters. The C_3H_8 selectivity is relatively low compared to others. The highest C_3H_8 selectivity of 4.275% was obtained using a 15wt% magnesia nanoparticle, reaction temperature of 380^oC, and reactor pressure of 4.275 bar. Most of the predicted values of the C_3H_8 selectivity are in proximity with the actual values. The R^2 value of 0.630 shows that the support vector machine is not robust in predicting the C_3H_8 selectivity as only 63% of the dataset can be learned with a prediction error of 0.806 as indicated by MSE. Figure 5 (b) depicts the dispersion plots showing the comparison between the actual and predicted C_3H_6 selectivity for every data point. The highest C_3H_6 selectivity of 19.4% is obtained using 25wt% magnesia nanoparticles, reaction temperature of 280^oC, and reactor pressure of 4 bar. Similar to the C_3H_8 selectivity, the prediction of the C_3H_6 selectivity resulted in R^2 of 0.610 and predictor error of 0.350%. The support vector machine needs to be optimised for an improved prediction of the C_3H_6 selectivity. The dispersion plot showing the comparison between the actual and predicted C_4H_8 selectivity is depicted in Figure 4 (c). Similar to C_3H_8 selectivity, and C_3H_6 selectivity, the C_4H_8 selectivity also has uneven distribution across the data points. It can be seen that a very low C_4H_8 selectivity was obtained at data points 9, 10, and 11, which could be attributed to the unfavourable reaction conditions for the C_4H_8 selectivity. The magnesia nanoparticles show the lowest selectivity towards C_4H_8. The highest C_4H_8 selectivity of 2.1% was obtained using 15wt% magnesia nanoparticles, reaction temperature of 380^oC, reactor pressure of 7 bar. The C_4H_8 selectivity is poorly predicted as indicated by the R^2 of 0.320 and predicted error of 7.231%. Only 32% of the dataset can be learned for the prediction of the C_4H_8 selectivity (Table 1). Therefore, the support

Table 1: Summary of the prediction performance of the support vector machine

Performance Metrics	*CO conversion*	*CH_4 selectivity*	*C_2H_6 selectivity*	*C_2H_4 selectivity*	*C_3H_8 selectivity*	*C_4H_8 selectivity*	*C_3H_6 selectivity*
RMSE	3.875	3.291	1.807	1.807	0.897	0.591	2.689
R^2	0.770	0.800	0.730	0.930	0.630	0.610	0.320
MSE	15.018	10.830	3.266	2.809	0.806	0.350	7.231
MAE	2.934	2.778	1.627	1.572	0.616	0.410	2.352

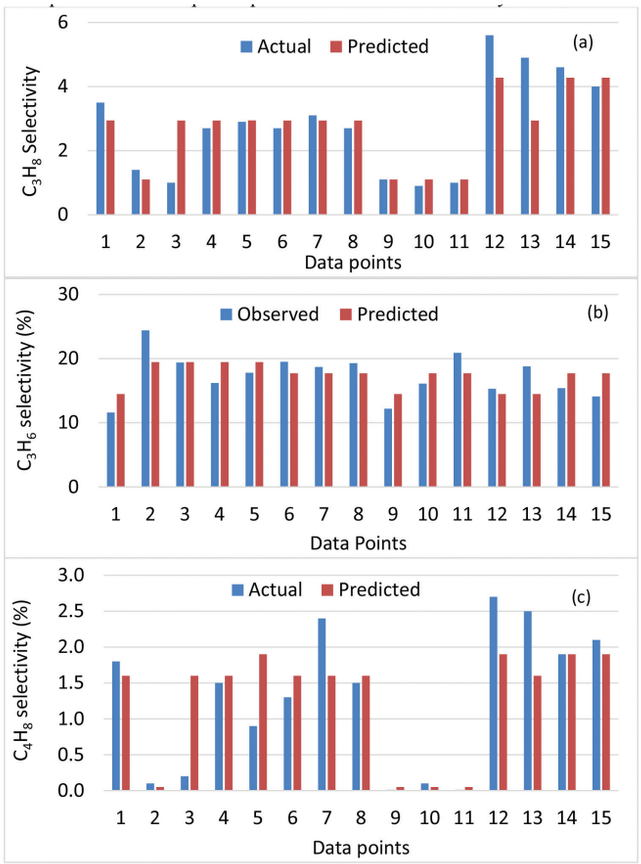

Figure 5: Dispersion plots showing the comparison between (a) the actual and predicted C_3H_8 selectivity, (b) the actual and predicted C_3H_6 selectivity and (c) the actual and predicted C_4H_8 selectivity.

vector machine algorithms need to be optimised for an improved prediction of the C_4H_8 selectivity.

Conclusion

This study has demonstrated the potential of employing a support vector machine with fine Gaussian kernel function for predictive modeling of CO conversion and light olefin during CO hydrogenation reaction. The CO conversion and the selectivity of the light olefins show significant variation along with the data points due to differences in the combined parameters. The performance of the fine Gaussian kernel support vector machine in predicting the CO conversion and the light olefins varies across the data points. A significant predictive ability was displayed by the support vector machine during the prediction of CO conversion, CH_4 selectivity, C_2H_6 selectivity, and C_2H_4 selectivity as indicated by R^2 of 0.770, 0.800, 0.730, and 0.930, respectively. Whereas less predictive performance was obtained for the prediction of C_3H_8 selectivity, C_4H_8 selectivity, and C_3H_6 selectivity as indicated by R^2 of 0.630, 0.610, and 0.320, respectively.

Acknowledgement

The authors acknowledge the financial support of the Department of Chemical Engineering, University of Technology, Iraq.

References

Atashi, H., Shiva, M., Farshchi Tabrizi, F. and A.A. Mirzaei (2013). Study of syngas conversion to light olefins by response surface methodology. *Journal of Chemistry*, 2013. https://doi.org/10.1155/2013/945735

Azapagic, A., Stamford, L., Youds, L. and C. Barteczko-Hibbert (2016). Towards sustainable production and consumption: A novel DEcision-Support Framework IntegRating Economic, Environmental and Social Sustainability (DESIRES). *Computers & Chemical Engineering*, **91:** 93-103. https://doi.org/https://doi.org/10.1016/j.compchemeng.2016.03.017

Bai, Y., Sun, Z., Zeng, B., Long, J., Li, L., de Oliveira, J.V. and C. Li (2019). A comparison of dimension reduction techniques for support vector machine modeling of multi-parameter manufacturing quality prediction. *Journal of Intelligent Manufacturing*, **30(5):** 2245-2256. https://doi.org/10.1007/s10845-017-1388-1

Corma, A., Corresa, E., Mathieu, Y., Sauvanaud, L., Al-Bogami, S., Al-Ghrami, M. S. and A. Bourane (2017). Crude oil to chemicals: Light olefins from crude oil. *Catalysis Science and Technology*, **7(1):** 12-46. https://doi.org/10.1039/c6cy01886f

Fan, J., Wu, L., Zhang, F., Cai, H., Wang, X., Lu, X. and Y. Xiang (2018). Evaluating the effect of air pollution on global and diffuse solar radiation prediction using support vector machine modeling based on sunshine duration and air temperature. *Renewable and Sustainable Energy Reviews*, **94:** 732-747. https://doi.org/https://doi.org/10.1016/j.rser.2018.06.029

Ji, X., Shang, X., Dahlgren, R.A. and M. Zhang (2017). Prediction of dissolved oxygen concentration in hypoxic river systems using support vector machine: a case study of Wen-Rui Tang River, China. *Environmental Science and Pollution Research*, **24(19):** 16062-16076. https://doi.org/10.1007/s11356-017-9243-7

Leong, W.C., Bahadori, A., Zhang, J. and Z. Ahmad (2021). Prediction of water quality index (WQI) using support vector machine (SVM) and least square-support vector machine (LS-SVM). *International Journal of River Basin*

Management, **19(2):** 149-156. https://doi.org/10.1080/15715124.2019.1628030

Mohammadi, N., Samimi, A., Antalovits, F., Niedzwiecki, L. and R. Mesbah (2021). Optimization of operating conditions for CO hydrogenation to hydrocarbon via response surface method. *Chemical Methodologies*, **5:** 178-189. https://doi.org/10.22034/chemm.2021.122477

Pedersen, E.Ø., Svenum, I.-H. and E.A. Blekkan (2018). Mn promoted Co catalysts for Fischer-Tropsch production of light olefins – An experimental and theoretical study. *Journal of Catalysis*, **361:** 23-32. https://doi.org/https://doi.org/10.1016/j.jcat.2018.02.011

Rădulescu, M., Rădulescu, S. and C.Z. Rădulescu (2009). Sustainable production technologies which take into account environmental constraints. *European Journal of Operational Research*, **193(3):** 730-740. https://doi.org/https://doi.org/10.1016/j.ejor.2007.05.057

Shi, B., Zhang, Z., Liu, Y., Su, J., Liu, X., Li, X., Wang, J., Zhu, M., Yang, Z., Xu, J. and Y.-F. Han (2020). Promotional effect of Mn-doping on the structure and performance of spinel ferrite microspheres for CO hydrogenation. *Journal of Catalysis*, **381:** 150-162. https://doi.org/https://doi.org/10.1016/j.jcat.2019.10.034

Wang, Y., Zhao, Y., Liu, J., Li, Z., Waterhouse, G.I.N., Shi, R., Wen, X. and T. Zhang (2020). Manganese oxide modified nickel catalysts for photothermal CO hydrogenation to light olefins. *Advanced Energy Materials*, **10(5):** 1-9. https://doi.org/10.1002/aenm.201902860

Yang, Z., Zhang, Z., Liu, Y., Ding, X., Zhang, J., Xu, J. and Y. Han (2021). Tuning direct CO hydrogenation reaction over Fe-Mn bimetallic catalysts toward light olefins: Effects of Mn promotion. *Applied Catalysis B: Environmental*, **285(November 2020):** 119815. https://doi.org/10.1016/j.apcatb.2020.119815

Yuan, X., Tan, Q., Lei, X., Yuan, Y. and X. Wu (2017). Wind power prediction using hybrid autoregressive fractionally integrated moving average and least square support vector machine. *Energy*, **129:** 122-137. https://doi.org/10.1016/j.energy.2017.04.094

Zendehboudi, A., Baseer, M.A. and R. Saidur (2018). Application of support vector machine models for forecasting solar and wind energy resources: A review. *Journal of Cleaner Production*, **199:** 272-285. https://doi.org/https://doi.org/10.1016/j.jclepro.2018.07.164

Zhu, Y., Pan, X., Jiao, F., Li, J., Yang, J., Ding, M., Han, Y., Liu, Z. and X. Bao (2017). Role of manganese oxide in syngas conversion to light olefins. *ACS Catalysis*, **7(4):** 2800-2804. https://doi.org/10.1021/acscatal.7b00221